Activation of integrin β-subunit I-like domains by one-turn C-terminal α-helix deletions

Wei Yang*†, Motomu Shimaoka*‡, JianFeng Chen*†, and Timothy A. Springer*†§

*CBR Institute for Biomedical Research and Departments of †Pathology and ‡Anesthesia, Harvard Medical School, 200 Longwood Avenue, Boston, MA 02115

Contributed by Timothy A. Springer, December 2, 2003

Integrins contain two structurally homologous but distantly related domains: an I-like domain that is present in all β-subunits and an I domain that is present in some α-subunits. Atomic resolution and mutagenesis studies of α I domains demonstrate a C-terminal, axial displacement of the α7-helix that allosterically regulates the shape and affinity of the ligand-binding site. Atomic resolution studies of β I-like domains have thus far demonstrated no similar α7-helix displacement; however, other studies are consistent with the idea that α I and β I-like domains undergo structurally analogous rearrangements. To test the hypothesis that C-terminal, axial displacement of the α7-helix, coupled with β6–α7 loop reshaping, activates β I-like domains, we have mimicked the effect of α7-helix displacement on the β6–α7 loop by shortening the α7-helix by two independent, four-residue deletions of about one turn of α-helix. In the case of integrin $\alpha_L\beta_2$, each mutant exhibits constitutively high affinity for the physiological ligand intercellular adhesion molecule 1 and full exposure of a β I-like domain activation-dependent antibody epitope. In the case of analogous mutants in integrin $\alpha_4\beta_7$, each mutant shows the activated phenotype of firm adhesion, rather than rolling adhesion, in shear flow. The results show that integrins that contain or lack α I domains share a common pathway of β I-like domain activation, and they suggest that β I-like and α I domain activation involves structurally analogous α7-helix axial displacements.

Integrins are large heterodimeric adhesion molecules that convey signals bidirectionally across the plasma membrane (1, 2). The extracellular domains exist in at least three global conformational states that differ in affinity for ligand (3, 4). Equilibria relate extracellular domain conformation to the separation between the α- and β-subunit cytoplasmic domains and the binding of these domains to cytoskeletal components, such as talin (3, 5–7). The key regulatory extracellular domain is the I-like domain of the β-subunit (3, 4, 8–10). The I-like domain contains three metal ion-binding sites (11, 12). The central metal ion-dependent adhesion site (MIDAS) metal ion ligates ligands directly (12, 13). At the outer ligand-induced metal-binding site and the adjacent to MIDAS (ADMIDAS) site, metal ions positively and negatively regulate affinity, respectively (13, 14). mAbs that either activate or inhibit ligand binding by β_1 integrins bind to almost-identical overlapping epitopes on the β_1 I-like domain (8), suggesting that these mAbs allosterically regulate the I-like domain, and mAbs to the β_2 I-like domain allosterically inhibit ligand binding by $\alpha_L\beta_2$ (10).

How bistability of the I-like domain is communicated conformationally to other domains is unknown and controversial. Here, we test the hypothesis that the mechanism is similar to that in the structurally homologous, but evolutionarily distantly related, I domain that is present in some integrin α-subunits. In α I domains, one- and two-turn axial displacements in the C-terminal direction of the α7-helix are linked to reshaping of the β6–α7 loop, rearrangements in the ligand-binding site around the MIDAS (15–17), and increases in affinity for ligand of up to 10,000-fold (17, 18). Two crystal structures of integrin $\alpha_V\beta_3$ in a bent conformation, in one of which a ligand-mimetic peptide was soaked, demonstrated no axial displacement of the α7-helix of the I-like domain, whereas other movements, including in the α1-helix, were present (11, 12). Therefore, it was concluded that conformational regulation of integrin β-subunit I-like domains differs from that of integrin α-subunit I domains in the absence of α7-helix displacement (12). Studies on an activation epitope in the β_1 I-like domain α1-helix that supported changes in this helix were also interpreted as suggesting a distinct activation mechanism for β I-like domains (19). Electron micrographic studies of integrins $\alpha_V\beta_3$ and $\alpha_5\beta_1$ demonstrate that ligand binding, in the absence of restraining crystal lattice contacts, induces a switchblade-like extension of the extracellular domain and a change in angle between the I-like and hybrid domains. Downward, axial displacement of the I-like α7-helix was suggested as the most plausible mechanism for linking ligand binding at the MIDAS to the change in angle at the interface with the hybrid domain (3, 4). Introduction of N-glycosylation wedges into the I-like hybrid domain interface designed to stabilize the active, swung-out conformation activated high-affinity ligand binding and integrin extension as predicted (20). Furthermore, the mapping of binding sites for activating mAbs to the inner side of the hybrid domain (21) and the results of solution x-ray scattering on the $\alpha_5\beta_1$ headpiece bound to a fibronectin fragment (14) are consistent with the direct observations of hybrid domain swing-out in the high-affinity ligand-bound integrin conformation (3, 4). Moreover, an activating mutation in the β_1 I-like α7-helix supports the notion that this region is allosterically important (21).

We are unaware of any studies that have tested the key hypothesis that axial displacement in the C-terminal direction of the β I-like domain α7-helix is activating, i.e., that α I and β I-like domains are activated by structurally homologous mechanisms. One prediction implied by this hypothesis is that shortening of the α7-helix by deletion of helical turns should pull the β6–α7 loop downward and have an activating effect on the I-like domain MIDAS-bearing face analogous to downward axial displacement of the α7-helix (Fig. 1). Here, we demonstrate that one-turn deletions of this α-helix in the integrin β_2- and β_7-subunits are activating, and we provide support for the hypothesis that C-terminal axial displacement of the I-like α7-helix activates two different integrins, one of which ($\alpha_L\beta_2$) contains an α I domain and the other of which ($\alpha_4\beta_7$) does not. The results support similar shape-shifting mechanisms for α I and β I-like domains.

Materials and Methods

Cell Lines, Antibodies, and Small Molecule Inhibitors. cDNAs of wild-type β_2 and β_7 were inserted into pcDNA3.1(+) or pcDNA3.1/Hygro(−) (Invitrogen) and used as the template for mutagenesis. Deletion mutants were generated by PCR overlap extension. Briefly, upstream and downstream primers were designed to include unique restriction sites. The restriction sites

Abbreviations: I-EGF*n*, integrin epidermal growth factor *n*; ICAM-1, intercellular adhesion molecule 1; MAdCAM-1, mucosal vascular addressin cell-adhesion molecule 1; MIDAS, metal ion-dependent adhesion site.

§To whom correspondence should be addressed. E-mail: springeroffice@cbr.med.harvard.edu.

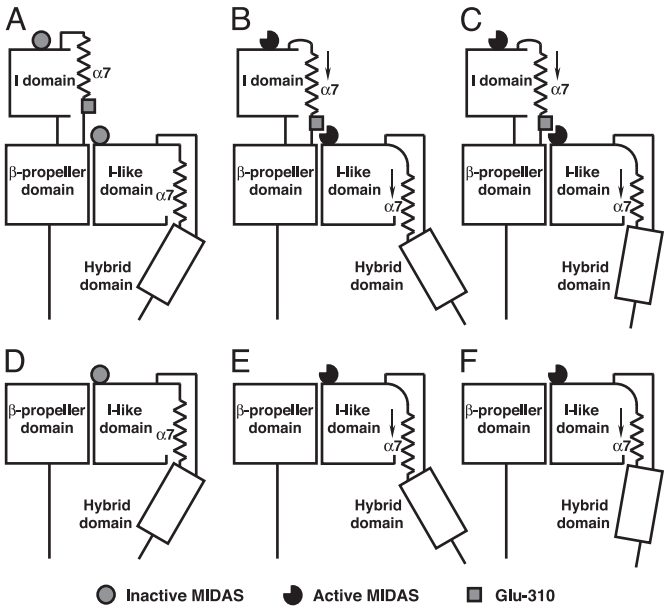

Fig. 1. Model of β I-like domain activation by axial, C-terminal α7-helix displacement and hybrid domain swing-out. Models for integrins containing (e.g., $\alpha_L\beta_2$; *A–C*) or lacking (e.g., $\alpha_4\beta_7$; *D–F*) I domains are shown. (*A*, *B*, *D*, and *E*) Downward movement of the β I-like α7-helix couples shape-shifting around the β MIDAS to hybrid domain swing-out. (*A* and *D*) Low-affinity state. (*B* and *E*) high-affinity state. (*C* and *F*) Shortening of the α7-helix by an integral number of turns is hypothesized to activate the high-affinity conformation of the MIDAS similarly, whereas it has a different effect on hybrid domain swing-out.

used in β_2 and β_7 were *Bsp*EI/*Sac*II and *Not*I/*Hin*dIII, respectively. Mutations were introduced by a pair of inner complementary primers. After a second round of PCR, the products were digested and ligated with the corresponding predigested plasmids. All constructs were verified by DNA sequencing. By using Lipofectamine 2000 (Invitrogen) according to manufacturer's instructions, 293T cells were transfected. K562 cells were transfected by electroporation and selected with 1 mg/ml G418 (22). mAbs to human α_L and β_2 were as described (10). The mAbs m24 (23) and KIM127 (24) were kind gifts from N. Hogg (Imperial Cancer Research Fund, London) and M. Robinson (Celltech, Slough, U.K.), respectively. KIM127 was biotinylated with EZ-Link Sulfo-NHS-LC-Biotin (Pierce), according to the manufacturer's instructions. LFA703 (25, 26) was obtained from Novartis Pharma (Basel). XVA143 (27) was synthesized according to example 345 of the patent (28) and was obtained also from Paul Gillespie (Roche).

Immunofluorescence Flow Cytometry. Immunofluorescence flow cytometry was performed as described (22). mAbs were used as 10 μg/ml purified IgG or 1:200 ascites. Binding of biotinylated KIM127 to cells was done in Hepes saline (20 mM Hepes, pH 7.5/140 mM NaCl), supplemented with ingredients as indicated at 37°C and detected by FITC-conjugated streptavidin (Zymed). Binding of m24 to cells was done in Hepes saline supplemented with ingredients as indicated at 4°C and detected by FITC-conjugated anti-mouse IgG (Zymed). Binding of other mAbs to cells was done in 2.5% FBS/L15 medium at 4°C and detected by FITC-conjugated anti-mouse IgG.

Cell Adhesion to Intercellular Adhesion Molecule 1 (ICAM-1). Binding of fluorescently labeled transfectants to immobilized ICAM-1 was done as described (22). Briefly, soluble ICAM-1 (domains 1–5) was purified from the culture supernatant of Chinese hamster ovary lec 3.2.8.1 transfectants and immobilized at 10 μg/ml on microtiter plates. Binding of 293T transfectants was in 2.5% FBS/L15 medium. Binding of K562 transfectants to immobilized ICAM-1 was determined in 20 mM Hepes, pH 7.5/140 mM NaCl/2 mg/ml glucose/1% BSA, supplemented with divalent cations and antibody as indicated. After incubation at 37°C for 30 min, unbound cells were washed off and bound cells were quantitated (22).

Binding of Soluble ICAM-1. Binding of soluble ICAM-1–IgA Fc fusion protein complexed with affinity-purified, FITC-conjugated anti-human IgA was measured by flow cytometry (29).

Adhesion to Mucosal Vascular Addressin Cell-Adhesion Molecule 1 (MAdCAM-1) in Shear Flow. Binding and rolling velocity of $\alpha_4\beta_7$ transfectants on MAdCAM-1 substrates was done in a parallel-plate flow chamber exactly as described (13).

Results

Design and Cell-Surface Expression of Mutant $\alpha_L\beta_2$ Integrin. We designed three β_2 mutants in which one or two turns of the C-terminal α7-helix of the I-like domain were deleted. In mutants β_2-4b and β_2-4a, a single turn of α-helix comprising the four β_2 residues 336–339 or 340–343 was deleted, respectively (Fig. 2*A*). In mutant β_2-7, two turns of α-helix comprising the seven β_2 residues 337–343 were deleted. Wild-type or mutated β_2-subunits were coexpressed with wild-type α_L-subunits in 293T cell transfectants. Immunofluorescence flow cytometry with TS2/4, a mAb that recognizes the α_L β-propeller domain only when it is associated with the β_2 I-like domain (30), demonstrated that the β_2-4a and β_2-4b mutants were expressed almost at wild-type levels, whereas the β_2-7 mutation abolished $\alpha_L\beta_2$ cell-surface expression (Fig. 2). The expression of other mAb epitopes was measured relative to TS2/4 expression (Fig. 2*B*). The mAbs May.017 and MHM23, which map to E175 in the specificity-determining loop between the β2- and β3-strands of the β_2 I-like domain, and CBR LFA-1/2, which maps to the β_2 integrin epidermal growth factor 3 (I-EGF3) domain (32, 33), all bind $\alpha_L\beta_2$-4a, $\alpha_L\beta_2$-4b, and wild-type $\alpha_L\beta_2$ equally well. The mAbs TS1/18 and YFC51, which map to residue R133 in the α1-helix and His-332 in the α7-helix of the β_2 I-like domain (Fig. 2*A*), bind well to $\alpha_L\beta_2$-4a but bind poorly to $\alpha_L\beta_2$-4b. This finding is readily explained by the location of the epitope residue His-332, which is two α-helix turns away from the 340–343 deletion in the $\alpha_L\beta_2$-4a mutant but only one turn away from the 336–339 deletion in the $\alpha_L\beta_2$-4b mutant (Fig. 2*B*). CLB LFA-1/1, which maps to residues His-332 and Asn-339 in the α7-helix of the β_2 I-like domain (Fig. 2*A*) did not bind either the $\alpha_L\beta_2$-4a or $\alpha_L\beta_2$-4b mutant. This result is explained by the location of Asn-339 in the region deleted in $\alpha_L\beta_2$-4b and immediately adjacent to residues 340–343 deleted in $\alpha_L\beta_2$-4a. The lack of disruption of epitopes that were not included in or adjacent to the deletions suggests that the structural integrity of the β_2 I-like domain and its association with the α_L-subunit were not disturbed.

One-Turn Deletions in the β_2 I-Like α7-Helix Constitutively Activate Integrin $\alpha_L\beta_2$. The 293T transfectants expressing wild-type $\alpha_L\beta_2$ basally adhere to ICAM-1 immobilized on plastic substrates, and adhesiveness is enhanced further by the activating mAb CBR LFA-1/2, which binds to the β_2 I-EGF3 domain (Fig. 3*A*). The $\alpha_L\beta_2$-4a and $\alpha_L\beta_2$-4b mutants constitutively adhered to immobilized ICAM-1 at high levels that were not further increased by CBR LFA-1/2 mAb (Fig. 3*A*). $\alpha_L\beta_2$ containing the α_L-K287C/K294C mutation with an engineered disulfide bond that locks the α_L I domain in the high-affinity open conformation (34) was used as a positive control (Fig. 3*A*). The high-affinity $\alpha_L\beta_2$-4a

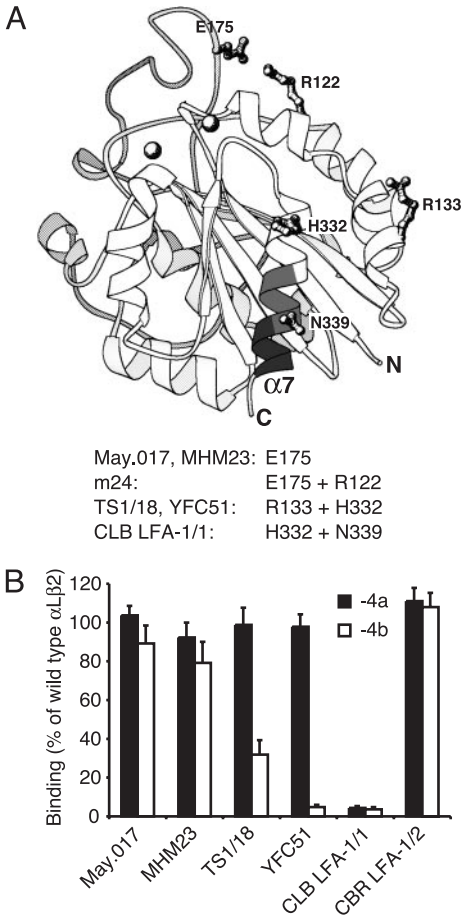

Fig. 2. Design and cell-surface expression of $\alpha_L\beta_2$ mutants with one-turn deletions in the α_7-helix of the β I-like domain. (*A*) Homology model of the β_2 I-like domain, which was created by using the β_3 I-like domain (ref. 12; Protein Data Bank ID code 1JV2) as template. The four-residue segments of the α_7-helix deleted in the β_2-4a and β_2-4b mutants are shown in dark gray and light gray, respectively. The side chains of species-specific residues that contribute to antibody epitopes are shown in ball-and-stick representation, and residues recognized by the antibodies are listed below the model (10, 31). The MIDAS (Protein Data Bank ID code 1L5G) and the metal-binding site adjacent to MIDAS metal ions are represented by left and right spheres, respectively. (*B*) Reactivity of mutants with mAb. The 293T cells transiently transfected with wild-type α_L and wild-type or mutant β_2 were stained with the indicated mAb and subjected to flow cytometry, and the specific mean fluorescence intensity (after intensity of mock transfectants was subtracted) was determined and divided by specific mean fluorescence intensity with TS2/4 mAb to the α_L β-propeller. Binding of TS2/4 mAb to the $\alpha_L\beta_2$-4a and -4b mutants was 47 $\pm$ 5% and 67 $\pm$ 6%, respectively, of binding to wild-type $\alpha_L\beta_2$. The percentage of the mutant/wild-type values is shown. Error bars show SD of three independent experiments.

and $\alpha_L\beta_2$-4b mutants showed the same behavior, with maximal adhesiveness that was not further increased by CBR LFA-1/2.

Residue α_L Glu-310 in the linker connecting the α_L I domain to the β-propeller domain is hypothesized to act as an intrinsic ligand that binds to the activated β_2 I-like domain and relays activation to the α_L I domain (2, 35–37). Consistent with this notion and the expectation that the activation of the β_2 I-like domain by β_2-4a and β_2-4b mutations would need to be relayed to the α_L I domain to activate adhesiveness to ICAM-1, the α_L-E310A mutation abolished adhesiveness by the β_2-4a and β_2-4b mutants (Fig. 3*A*). Similarly, CBR LFA-1/2-stimulated adhesiveness of wild-type $\alpha_L\beta_2$ was abolished in α_L-E310A/β_2 mutants (Fig. 3*A*).

The function of the β_2-4a mutant was studied further in stable

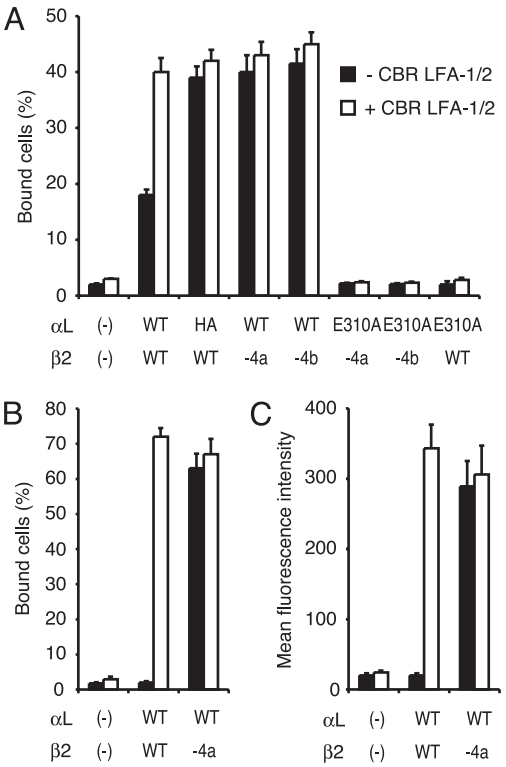

Fig. 3. Ligand-binding activity of $\alpha_L\beta_2$ mutants. (*A*) Binding of 293T cell transient transfectants to immobilized ICAM-1. Adhesion to ICAM-1 of cells transfected with the indicated α_L and β_2 cDNA was determined in the absence (filled bars) or presence (open bars) of the activating mAb CBR LFA-1/2 at 37°C. high-affinity (HA) α_L K287C/K294C I domain mutant (34). The $\alpha_L\beta_2$-4a and $\alpha_L\beta_2$-4b mutants were expressed slightly less well than the other $\alpha_L\beta_2$ complexes, but data are not normalized. (*B* and *C*) Binding of K562 stable transfectants to immobilized ICAM-1 (*B*) and soluble ICAM-1 complexes (*C*). Binding was assayed in the presence of 1 mM $CaCl_2$/1 mM $MgCl_2$ (filled bars) or 2 mM $MnCl_2$/10 μg/ml CBR LFA-1/2 mAb (open bars) at room temperature. Error bars show SD of three independent experiments. $\alpha_L\beta_2$-4a was expressed on K562 transfectants 106 $\pm$ 9% as well as wild-type (WT) $\alpha_L\beta_2$, as shown by staining with TS2/4.

K562 transfectants expressing identical amounts of wild-type $\alpha_L\beta_2$ and $\alpha_L\beta_2$-4a. Wild-type $\alpha_L\beta_2$ expressed in K562 cells showed little basal adhesion to immobilized ICAM-1 (Fig. 3*B*) or binding to soluble, multimeric ICAM-1 (Fig. 3*C*), whereas adhesion and binding was greatly increased by the activating mAb CBR LFA-1/2 and Mn^{2+} (Fig. 3 *B* and *C*). By contrast, K562 cells expressing $\alpha_L\beta_2$-4a strongly adhered to immobilized ICAM-1 and bound soluble ICAM-1 even in the absence of activation (Fig. 3 *B* and *C*). The binding appeared to be maximal because it was not increased further by CBR LFA-1/2 mAb and Mn^{2+} and was as high as binding by wild-type $\alpha_L\beta_2$ activated with CBR LFA-1/2 mAb and Mn^{2+}. The data described above demonstrate clearly that one-turn deletions in the C-terminal α7-helix of the β_2 I-like domain fully activate ligand binding by $\alpha_L\beta_2$.

Impact of One-Turn Deletions on Activation Epitopes in the β_2 I-Like and I-EGF2 Domains. The active conformation of the β_2 I-like domain is reported by the mAb m24, which recognizes the species-specific residues Arg-122 in the α1-helix and Glu-175 in the specificity-determining loop of the β_2 I-like domain (10, 23, 38) (Fig. 2*A*). The extended conformation of the β_2-subunit is detected by the mAb KIM127, which maps to species-specific residues in the I-EGF2 domain that are buried in the headpiece–tailpiece interface in the bent integrin conformation and ex-

CELL BIOLOGY

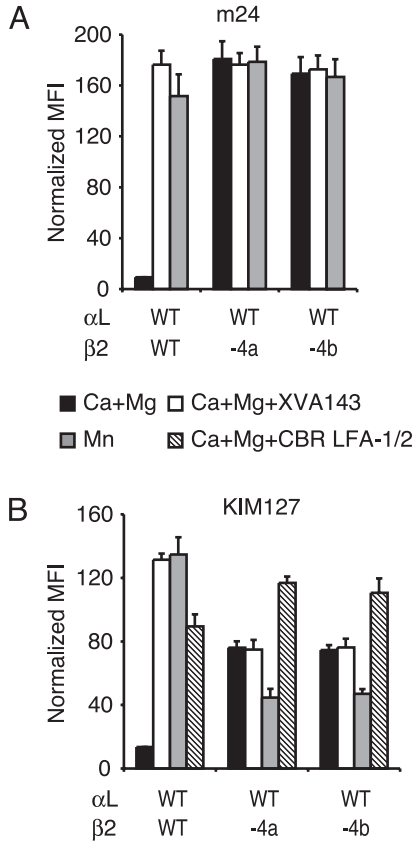

Fig. 4. Exposure of activation epitopes. Transient transfectants of 293T cells were stained with m24 mAb (*A*) or biotinylated KIM127 mAb (*B*) with the indicated additions. Binding of m24 was detected by FITC-conjugated anti-mouse IgG. Binding of KIM127 was detected by FITC-conjugated streptavidin. Specific mean fluorescence intensity (MFI) was normalized by dividing by the ratio of mutant/wild-type (WT) TS2/4 mAb mean fluorescence intensity. Error bars show SD of three independent experiments.

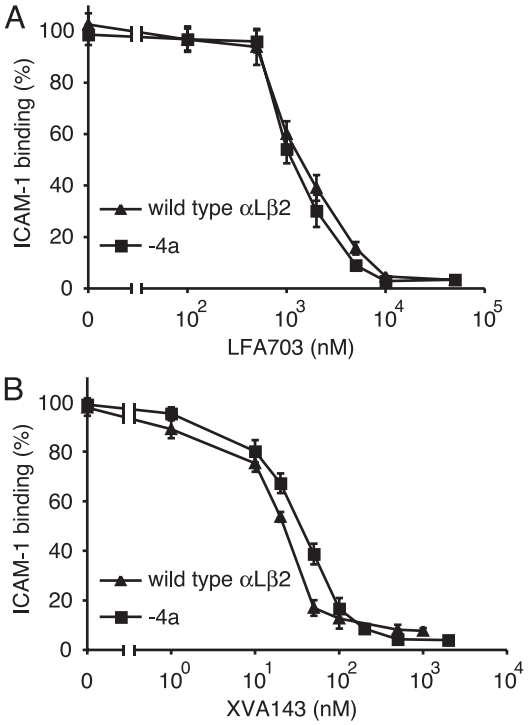

Fig. 5. Inhibition by small molecule antagonists of binding to ICAM-1. Wild-type and mutant K562 transfectants were assayed with and without preactivation with the mAb CBR LFA-1/2, respectively. Binding to soluble, multimeric ICAM-1 in medium containing 1 mM $CaCl_2$ and 1 mM $MgCl_2$ was done in the presence of LFA703 (*A*) or XVA143 (*B*). Data represent mean ± SD of three different experiments.

posed in the extended conformation (32, 39). Both m24 and KIM127 bound poorly to wild-type $\alpha_L\beta_2$ in Ca^{2+}/Mg^{2+} (Fig. 4), and both mAbs bound well to wild-type $\alpha_L\beta_2$ in the presence of Mn^{2+}, which activates $\alpha_L\beta_2$ (Fig. 4). Binding of the biotin-labeled KIM127 mAb was measured also in the presence of CBR LFA-1/2 mAb, which markedly enhanced binding to wild-type $\alpha_L\beta_2$ (Fig. 4*B*). Expression of the m24 and KIM127 epitopes in wild-type $\alpha_L\beta_2$ was greatly induced also by the small molecule antagonist XVA143 (Fig. 4). XVA143 binds to the β_2 I-like domain MIDAS and induces the active conformation of the β_2 I-like domain and integrin extension, whereas it leaves the α I domain in a default inactive conformation by disrupting signal transmission between the α I and β I-like domains (27, 29). Both $\alpha_L\beta_2$-4a and $\alpha_L\beta_2$-4b showed maximal binding to m24 mAb without addition of activating agents, indicating that their I-like domains were in the fully activated state (Fig. 4*A*). $\alpha_L\beta_2$-4a and $\alpha_L\beta_2$-4b bound to KIM127 mAb substantially more than wild-type $\alpha_L\beta_2$, suggesting that they favor the extended conformation (Fig. 4*B*). However, exposure of the KIM127 epitope in $\alpha_L\beta_2$-4a and $\alpha_L\beta_2$-4b in Ca^{2+}/Mg^{2+} was not maximal because it was lower than wild-type $\alpha_L\beta_2$ activated by XVA143 or Mn^{2+} and could be further increased by CBR LFA-1/2 mAb (Fig. 4*B*). Consistent with maximum activation of the β_2 I-like domain in the mutants, XVA143 binding to this domain in the mutants did not further increase KIM127 epitope exposure (Fig. 4*B*). Therefore, maximal I-like domain activation in the mutants is coupled to partial, but not maximal, integrin extension as measured by KIM127 epitope exposure, consistent with the predicted difference in hybrid domain swing-out between activated wild-type $\alpha_L\beta_2$ and mutant $\alpha_L\beta_2$-4a and $\alpha_L\beta_2$-4b integrins (Fig. 1 *A* and *B*). Curiously, Mn^{2+} enhanced KIM127 exposure in wild-type $\alpha_L\beta_2$ but diminished it in the $\alpha_L\beta_2$-4a and $\alpha_L\beta_2$-4b mutants (Fig. 4*B*).

Susceptibility to Small-Molecule Antagonists and Inhibitory Antibodies. α I and α/β I-like allosteric antagonists have distinct mechanisms of inhibition and binding sites on $\alpha_L\beta_2$ (29). LFA703 is an α I allosteric antagonist that binds to the hydrophobic pocket underneath the C-terminal α7-helix of the α_L I domain and stabilizes the I domain in its closed conformation (25, 26, 34). With the same potency, LFA703 inhibited the constitutive binding to soluble ICAM-1 by $\alpha_L\beta_2$-4a K562 transfectants and the binding to soluble ICAM-1 by wild-type $\alpha_L\beta_2$ transfectants induced by pretreatment with CBR LFA-1/2 mAb (Fig. 5*A*). Similar results were obtained with the α/β I-like allosteric antagonist XVA143 (Fig. 5*B*). Thus, activation of the α_L I domain by the mutationally activated β_2 I-like domain can be blocked by stabilizing the closed conformation of the α_L I domain with LFA703 or by blocking communication between the β_2 I-like domain MIDAS and the α_L I domain with XVA143.

Inhibitory mAbs to both the α_L I domain and β_2 I-like domain were tested similarly for inhibition of binding to multimeric ICAM-1 by $\alpha_L\beta_2$ mutants and by CBR LFA-1/2-activated wild-type $\alpha_L\beta_2$. Ligand binding by $\alpha_L\beta_2$-4a was inhibited by all tested mAbs to the α_L I domain (Table 1). All tested mAbs to the β_2 I-like domain, and some to the α_L I domain, inhibit by an allosteric mechanism, as confirmed by lack of inhibition of high-affinity $\alpha_L\beta_2$ with the locked open α_L I domain (10) (Table 1). All tested mAbs to the β_2 I-like domain except CLB LFA-1/1, which does not bind to $\alpha_L\beta_2$-4a, inhibited both wild-type $\alpha_L\beta_2$ and the $\alpha_L\beta_2$-4a mutant. This finding suggests that the one-turn

Table 1. Inhibition by α_L I and β_2 I-like domain antibodies of multimeric ICAM-1 binding to $\alpha_L\beta_2$

mAb	Domain	Epitope	Inhibition (%)		
			Wild-type $\alpha_L\beta_2$	$\alpha_L\beta_2$-4a	HA$\alpha_L\beta_2$*
TS2/6	α_L I	154–183	97	97	97
May.035	α_L I	K197,H201	98	97	97
MHM24	α_L I	K197	96	98	96
TS1/22	α_L I	Q266,S270	96	96	92
TS2/14	α_L I	S270,E272	99	97	14
CBR LFA-1/1	α_L I	301–338	97	96	2
May.017	β_2 I-like	E175, ?	98	97	3
MHM23	β_2 I-like	E175	97	93	2
TS1/18	β_2 I-like	R133,H332	98	88	0
YFC51	β_2 I-like	R133,H332	98	87	0
CLB LFA-1/1†	β_2 I-like	H332,N339	97	2	0

Wild-type and mutant K562 transfectants were assayed with and without preactivation with mAb CBR LFA-1/2, respectively. Binding to soluble, multimeric ICAM-1 in medium containing 1 mM $CaCl_2$ and 1 mM $MgCl_2$ in the presence of the indicated mAb was assayed by immunofluorescence flow cytometry. Results are given as means of three experiments.

*$\alpha_L\beta_2$ with the high-affinity K287C/K294C I domain mutation (34).

†Binding of CLB LFA-1/1 to the $\alpha_L\beta_2$-4a mutant was <5% of binding to wild-type $\alpha_L\beta_2$. All other mAbs bound to $\alpha_L\beta_2$-4a, high-affinity $\alpha_L\beta_2$, and wild-type $\alpha_L\beta_2$ transfectants equally well.

deletion does not activate the β_2 I-like domain irreversibly and that allosteric, inhibitory mAbs to the I-like domain can still shift the conformational equilibrium toward the inactive form of the I-like domain.

Generalization to the Integrin $\alpha_4\beta_7$. One-turn deletions were made in the α7-helix of the β_7 I-like domain to generalize the findings described above to an integrin that lacks an α I domain, $\alpha_4\beta_7$. Deletions of residues 369–372 and 365–368 were made in the β_7-4a and β_7-4b mutants, respectively, in positions homologous to those deleted in the β_2 mutants. The behavior of $\alpha_4\beta_7$ transfectants was tested in parallel-wall flow chambers bearing the ligand MAdCAM-1 adsorbed to substrates that formed the lower wall of the chamber. As demonstrated in refs. 13 and 39, in the resting state in Ca^{2+} or Ca^{2+} plus Mg^{2+}, wild-type $\alpha_4\beta_7$ mediates rolling adhesion, whereas in the activated state in Mn^{2+}, $\alpha_4\beta_7$ mediates firm adhesion (Fig. 6). By contrast, $\alpha_4\beta_7$-4a and $\alpha_4\beta_7$-4b transfectants were firmly adherent in Ca^{2+} plus Mg^{2+} as well as Mn^{2+} (Fig. 6), demonstrating that each of the one-turn deletions was activating.

Discussion

The β I-like domain directly binds ligand in integrins that lack α I domains, and it indirectly regulates ligand binding by integrins that contain α I domains. It plays an important role in bistable regulation of integrin activity (13). However, as reviewed in the Introduction, it is still controversial whether β-subunit I-like domains and α-subunit I domains are activated by structurally analogous mechanisms. Mutational and structural studies on α I domains have demonstrated that C-terminal axial displacement, i.e., "downward" movement of the α7-helix, is allosterically linked to rearrangements of the α I MIDAS and its surrounding loops into the high-affinity ligand-binding conformation. Mutational and structural studies on the α_L I domain have shown that the conformation of the α7-helix *per se* is not important for allostery but rather that reshaping of the ligand-binding site is linked directly to the downward movement and reshaping of the β6–α7 loop that is induced by α7-helix displacement (17). Furthermore, two reshapings of the β6–α7 loop that correspond to one- and two-turn α_7-helix displacements have been visualized in α_L I domain mutants with intermediate and high affinity for ligand, respectively (17). Because deletion of integral numbers of turns of the α7-helix and downward displacement of the α7-helix should have similar affects on reshaping of the β6–α7 loop, we tested the hypothesis that α I and β

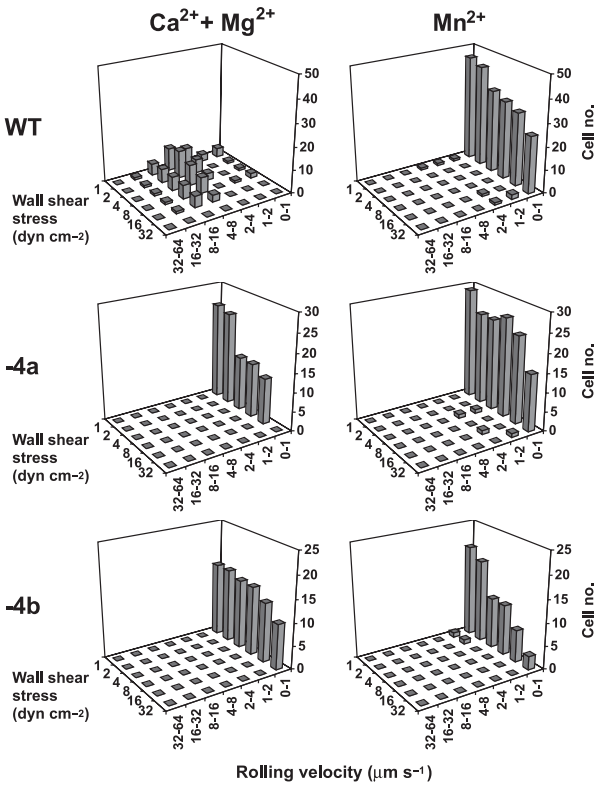

Fig. 6. Rolling velocity of $\alpha_4\beta_7$ 293T cell transfectants on MAdCAM-1 substrates in shear flow. Cells were infused into the parallel-wall flow chamber in 1 mM Ca^{2+}/1 mM Mg^{2+} or 2 mM Mn^{2+}, as indicated. Rolling velocities of individual cells were measured as a series of increasing wall-shear stresses (in dyne/cm^{-2}; 1 dyne = 10 μN), and cells within a given velocity range were enumerated to yield the population distribution. $\alpha_4\beta_7$-4a and $\alpha_4\beta_7$-4b were expressed on transfectants 17% and 11%, respectively, as well as wild-type $\alpha_4\beta_7$, as shown by staining with Act-1 mAb to $\alpha_4\beta_7$.

I-like domains are activated by structurally homologous mechanisms by making deletions in the β I-like α7-helix.

Our results demonstrate that the α7-helix has a key role in β I-like domain activation. Two distinct, nonoverlapping α7-helix deletions of four residues, i.e., about one α-helical turn, were each fully activating in the β_2 I-like domain. Similar results were obtained with nonoverlapping four-residue deletions in the α7-helix of the I-like domain of the β7-subunit. These results suggest strongly that C-terminal α7-helix displacement *per se*, rather than specific interactions of α7-helix residues with other I-like domain residues, regulates activation. Introduction of disulfide bonds into the β6–α7 loop of the β_3 I-like domain also suggests that downward movement of the α7-helix activates ligand binding by integrin $\alpha_{IIb}\beta_3$ (41).

The full exposure of the m24 epitope, which maps to residues near the MIDAS on the "top" face of the β_2 I-like domain, suggests strongly that the effect of α7-helix shortening, which was carried out on the C-terminal, or "bottom" portion of the α7-helix, was conveyed conformationally to the top face of the I-like domain, suggesting that β6–α7 loop reshaping occurred. The full activation of ligand binding by $\alpha_L\beta_2$ and $\alpha_4\beta_7$, and the lack of any further effect of XVA143 binding, suggest strongly that the high-affinity conformation of the I-like MIDAS region was achieved. Thus, conformational change in the "upward" direction toward the ligand-binding interfaces occurred. Some change in the downward direction toward the KIM127 epitope in the β_2 I-EGF2 domain also occurred; however, this change was lesser because the KIM127 epitope was not exposed fully.

The β_2 I-like domain did not appear to be irreversibly activated by α7-helix shortening because mAbs that bind to and allosterically regulate the I-like domain could still inhibit ligand binding by $\alpha_L\beta_2$. Recently, we have made similar observations with the α I domain; the effect of certain mutations that "pull down" the α_L I domain α7-helix can be reversed by allosteric modulators (42). Thus, both the α I domain and β I-like domain α7-helices should be viewed not as stiff rods but more as pull springs that are capable of some elastic deformation.

In summary, we have shown that one-turn deletions of the β_2 and β_7 I-like domain α_7-helices fully activate ligand binding by the $\alpha_L\beta_2$ and $\alpha_4\beta_7$ integrins, demonstrating that integrins that contain I domains and those that lack I domains share a common pathway of I-like domain activation. Furthermore, our results suggest that the integrin β-subunit I-like domain activation pathway involves a one-turn, axial displacement in the C-terminal direction of the α7-helix and is structurally analogous to integrin α-subunit I domain activation, which involves C-terminal, axial displacement of one or two turns of the α7-helix.

We thank Drs. Junichi Takagi and Daniel Leahy for reviewing the manuscript. This work was supported by National Institutes of Health Grant CA31798.

1. Hynes, R. O. (2002) *Cell* **110,** 673–687.
2. Shimaoka, M., Takagi, J. & Springer, T. A. (2002) *Annu. Rev. Biophys. Biomol. Struct.* **31,** 485–516.
3. Takagi, J., Petre, B. M., Walz, T. & Springer, T. A. (2002) *Cell* **110,** 599–611.
4. Takagi, J., Strokovich, K., Springer, T. A. & Walz, T. (2003) *EMBO J.* **22,** 4607–4615.
5. Vinogradova, O., Velyvis, A., Velyviene, A., Hu, B., Haas, T. A., Plow, E. F. & Qin, J. (2002) *Cell* **110,** 587–597.
6. Kim, M., Carman, C. V. & Springer, T. A. (2003) *Science* **301,** 1720–1725.
7. Tadokoro, S., Shattil, S. J., Eto, K., Tai, V., Liddington, R. C., de Pereda, J. M., Ginsberg, M. H. & Calderwood, D. A. (2003) *Science* **302,** 103–106.
8. Takada, Y. & Puzon, W. (1993) *J. Biol. Chem.* **268,** 17597–17601.
9. Mould, A. P., Akiyama, S. K. & Humphries, M. J. (1996) *J. Biol. Chem.* **271,** 20365–20374.
10. Lu, C., Shimaoka, M., Zang, Q., Takagi, J. & Springer, T. A. (2001) *Proc. Natl. Acad. Sci. USA* **98,** 2393–2398.
11. Xiong, J.-P., Stehle, T., Diefenbach, B., Zhang, R., Dunker, R., Scott, D. L., Joachimiak, A., Goodman, S. L. & Arnaout, M. A. (2001) *Science* **294,** 339–345.
12. Xiong, J.-P., Stehle, T., Zhang, R., Joachimiak, A., Frech, M., Goodman, S. L. & Arnaout, M. A. (2002) *Science* **296,** 151–155.
13. Chen, J. F., Salas, A. & Springer, T. A. (2003) *Nat. Struct. Biol.* **10,** 995–1001.
14. Mould, A. P., Barton, S. J., Askari, J. A., Craig, S. E. & Humphries, M. J. (2003) *J. Biol. Chem.*, **278,** 51622–51629.
15. Lee, J.-O., Bankston, L. A., Arnaout, M. A. & Liddington, R. C. (1995) *Structure (London)* **3,** 1333–1340.
16. Emsley, J., Knight, C. G., Farndale, R. W., Barnes, M. J. & Liddington, R. C. (2000) *Cell* **101,** 47–56.
17. Shimaoka, M., Xiao, T., Liu, J.-H., Yang, Y., Dong, Y., Jun, C.-D., McCormack, A., Zhang, R., Joachimiak, A., Takagi, J., *et al*. (2003) *Cell* **112,** 99–111.
18. Shimaoka, M., Lu, C., Palframan, R., von Andrian, U. H., Takagi, J. & Springer, T. A. (2001) *Proc. Natl. Acad. Sci. USA* **98,** 6009–6014.
19. Mould, A. P., Askari, J. A., Barton, S., Kline, A. D., McEwan, P. A., Craig, S. E. & Humphries, M. J. (2002) *J. Biol. Chem.* **277,** 19800–19805.
20. Luo, B.-H., Springer, T. A. & Takagi, J. (2003) *PNAS* **100,** 2403–2408.
21. Mould, A. P., Barton, S. J., Askari, J. A., McEwan, P. A., Buckley, P. A., Craig, S. E. & Humphries, M. J. (2003) *J. Biol. Chem.* **278,** 17028–17035.
22. Lu, C. & Springer, T. A. (1997) *J. Immunol.* **159,** 268–278.
23. Dransfield, I. & Hogg, N. (1989) *EMBO J.* **8,** 3759–3765.
24. Robinson, M. K., Andrew, D., Rosen, H., Brown, D., Ortlepp, S., Stephens, P. & Butcher, E. C. (1992) *J. Immunol.* **148,** 1080–1085.
25. Kallen, J., Welzenbach, K., Ramage, P., Geyl, D., Kriwacki, R., Legge, G., Cottens, S., Weitz-Schmidt, G. & Hommel, U. (1999) *J. Mol. Biol.* **292,** 1–9.
26. Weitz-Schmidt, G., Welzenbach, K., Brinkmann, V., Kamata, T., Kallen, J., Bruns, C., Cottens, S., Takada, Y. & Hommel, U. (2001) *Nat. Med.* **7,** 687–692.
27. Welzenbach, K., Hommel, U. & Weitz-Schmidt, G. (2002) *J. Biol. Chem.* **277,** 10590–10598.
28. Fotouhi, N., Gillespie, P., Guthrie, R., Pietranico-Cole, S. & Yun, W. (1999) *PCT Int. Appl.* (Hoffmann La Roche, Switzerland) p. WO0021920.
29. Shimaoka, M., Salas, A., Yang, W., Weitz-Schmidt, G. & Springer, T. A. (2003) *Immunity* **19,** 391–402.
30. Huang, C. & Springer, T. A. (1997) *Proc. Natl. Acad. Sci. U.S.A.* **94,** 3162–3167.
31. Huang, C., Zang, Q., Takagi, J. & Springer, T. A. (2000) *J. Biol. Chem.* **275,** 21514–21524.
32. Lu, C., Ferzly, M., Takagi, J. & Springer, T. A. (2001) *J. Immunol.* **166,** 5629–5637.
33. Takagi, J., Beglova, N., Yalamanchili, P., Blacklow, S. C. & Springer, T. A. (2001) *Proc. Natl. Acad. Sci. USA* **98,** 11175–11180.
34. Lu, C., Shimaoka, M., Ferzly, M., Oxvig, C., Takagi, J. & Springer, T. A. (2001) *Proc. Natl. Acad. Sci. USA* **98,** 2387–2392.
35. Huth, J. R., Olejniczak, E. T., Mendoza, R., Liang, H., Harris, E. A., Lupher, M. L., Jr., Wilson, A. E., Fesik, S. W. & Staunton, D. E. (2000) *Proc. Natl. Acad. Sci. USA* **97,** 5231–5236.
36. Takagi, J. & Springer, T. A. (2002) *Immunol. Rev.* **186,** 141–163.
37. Alonso, J. L., Essafi, M., Xiong, J.-P., Stehle, T. & Arnaout, M. A. (2002) *Curr. Biol.* **12,** R340–R342.
38. Kamata, T., Tieu, K. K., Tarui, T., Puzon-McLaughlin, W., Hogg, N. & Takada, Y. (2002) *J. Immunol.* **168,** 2296–2301.
39. Beglova, N., Blacklow, S. C., Takagi, J. & Springer, T. A. (2002) *Nat. Struct. Biol.* **9,** 282–287.
40. de Chateau, M., Chen, S., Salas, A. & Springer, T. A. (2001) *Biochemistry* **40,** 13972–13979.
41. Luo, B. -H., Takagi, J. & Springer, T. A. (2004) *J. Biol. Chem.* in press.
42. Yang, W., Shimaoka, M., Salas, A., Takagi, J. & Springer, T. A. (2004) *Proc. Natl. Acad. Sci. U.S.A.* in press.